



## Optimal schemes for dispersion compensation of standard monomode fiber based links

D. Breuer<sup>a</sup>, K. Jürgensen<sup>b</sup>, F. Küppers<sup>b</sup>, A. Mattheus<sup>b</sup>, I. Gabitov<sup>c,d</sup>,  
S.K. Turitsyn<sup>d,1</sup>

<sup>a</sup> Technische Universität Berlin Fachbereich 12, Fachgebiet Hochfrequenztechnik, Einsteinufer 25, D-10587 Berlin, Germany

<sup>b</sup> Deutsche Telekom AG, Technologiezentrum, Postfach 100003, D-64276 Darmstadt, Germany

<sup>c</sup> L.D. Landau Institute for Theoretical Physics, Kosygin St. 2, 117940 Moscow, Russia

<sup>d</sup> Institut für Theoretische Physik I, H.-H.-Universität Düsseldorf, Universitätsstrasse 1, 40225 Düsseldorf, Germany

Received 9 December 1996; revised 10 March 1997; accepted 3 April 1997

### Abstract

Different schemes of dispersion management for cascaded transmission systems composed of standard monomode fibers (SMFs) and dispersion compensating fibers have been studied considering the most essential boundary conditions for practical network design. Alternating ordering of the compensation sections is found to improve considerably the eye opening penalty for high amplifier spacings of 120 km. © 1997 Elsevier Science B.V.

One of the most promising methods of installing high capacity all-optical networks on the already existing SMF base is the use of dispersion compensating fibers (DCFs) (see e.g. Refs. [1–9]). These passive and broadband devices are superior for WDM systems, commercially available, easy to install and cascable in networks, indicating that at present the DCF technique can effectively compete with any other dispersion management approach. In recent experiments, transmission of  $16 \times 10$  Gbit/s through 1000 km SMF with  $z_a = 40$  km amplifier spacing (SMF) [3],  $16 \times 10$  Gbit/s through 531 km SMF with  $z_a = 60$  to 91 km [4] and of  $55 \times 20$  Gbit/s through 150 km SMF with  $z_a = 50$  km [5] has been realized.

To date network design is aiming to achieve SMF amplifier spacing above  $z_a = 100$  km in order to reduce the number of repeater stations. Higher input powers are required due to these extended lengths of SMF sections, thus, increasing the impact of nonlinearity. In this article, we study numerically different schemes of dispersion management for 10 Gbit/s transmission over 960 km of SMF

with  $z_a = 120$  km, periodically placed EDFAs and periodic compensation by additional DCFs. It is most desirable for practical network design to have just one DCF bobbin either before or behind each SMF section instead of distributing several DCF pieces in between two subsequent amplifier stations. Taking into account this boundary condition we demonstrate that distortion due to accumulation of Kerr nonlinearity can considerably be minimized by an alternating compensation scheme, thus allowing long amplifier spans  $z_a$ , high peak powers and large transmission length.

The transmission line under consideration is presented in Fig. 1. It consists of a laser transmitter emitting 25 ps hyp-sech-shaped pulses of 36 mW peak power at 1.55  $\mu$ m wavelength with 100 ps pulse separation (corresponding to 10 Gbit/s data rate), 8 in-line blocks, and a receiver. Each in-line block is composed of 120 km SMF and 24 km DCF, and EDFAs with 26.4 dB (after SMF) and 19.2 dB (after DCF) amplification to compensate for the fiber losses, respectively. The noise figure of each amplifier was set to 6 dB. The nonlinear refractive index has been chosen as  $n_2 = 3 \times 10^{-20}$  m<sup>2</sup>/W for both SMF and DCF. The SMF is characterized by  $\alpha^{(1)} = 0.22$  dB/km attenuation.

<sup>1</sup> E-mail: turitsyn@xerxes.thphy.uni-duesseldorf.de.

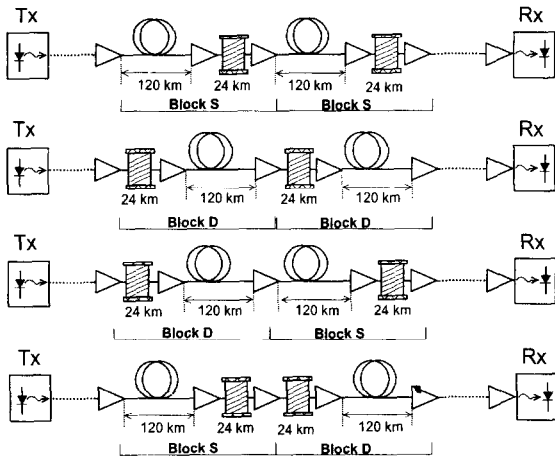


Fig. 1. Block diagrams of the transmission system design for different compensation schemes. Transmission line consists of the laser transmitter (Tx), in-line blocks and a receiver (Rx). Each block encompasses 120 km of SMF, 24 km DCF and the EDFAs to compensate for the fiber loss between consecutive amplifiers. The components within each block may be ordered in pre- and post-compensation scheme (denoted by D and S), respectively.

$D^{(1)} = 16.2 \text{ ps}/(\text{nm} \times \text{km})$  chromatic dispersion, and the effective fiber area  $A_{\text{eff}}^{(1)} = 95 \mu\text{m}^2$ , while we have  $\alpha^{(2)} = 0.8 \text{ dB}/\text{km}$ ,  $D^{(2)} = -81.0 \text{ ps}/(\text{nm} \times \text{km})$  and  $A_{\text{eff}}^{(2)} = 30 \mu\text{m}^2$  for DCF. Two basic alternative in-line blocks have been used reflecting pre- and post-compensation. We use notation S for a block with the SMF followed by an

EDFA, the DCF and the second EDFA, while D denotes the sequence DCF-EDFA-SMF-EDFA.

The pulse propagation was numerically simulated by the Split-Step Fourier Method, and the amplifier noise was modelled as a random Gaussian variable added to the electric field amplitude at the output of each amplifier, the results of simulations are presented in Figs. 2 and 3.

Firstly we have considered single pulse dynamics with different compensation schemes. Fig. 2a shows the pulse profile at the end of the link for the different configurations. Configurations DDDDDDDD and SSSSSSSS correspond to the pure pre- and post-compensations, respectively, while SDSDSDS and DSDSDSDS present alternating compensation schemes. In Fig. 2b the pulse width evolution along the line for the considered configurations is shown. A pulse dynamics in the single transmission block in the first approximation is as follows. On the first stage, the pulse width increases due to dispersive broadening and a pulse acquires a dispersion-induced frequency chirp. Entering a piece with another sign of dispersion the pulse compresses because of the accumulated chirp. During propagation the amplitude of the pulse is periodically regenerated at the end of each fiber piece. Due to nonadditive interplay of dispersive and nonlinear effects the pulse width is not entirely restored at the end of a compensation block. The important feature that we found in our simulations is that, after passing a pure post-compensated line, pulses are broadened and opposite, the pure pre-compensation scheme leads to an effective pulse compression. In both schemes the pulse is severely affected by fibre nonlin-

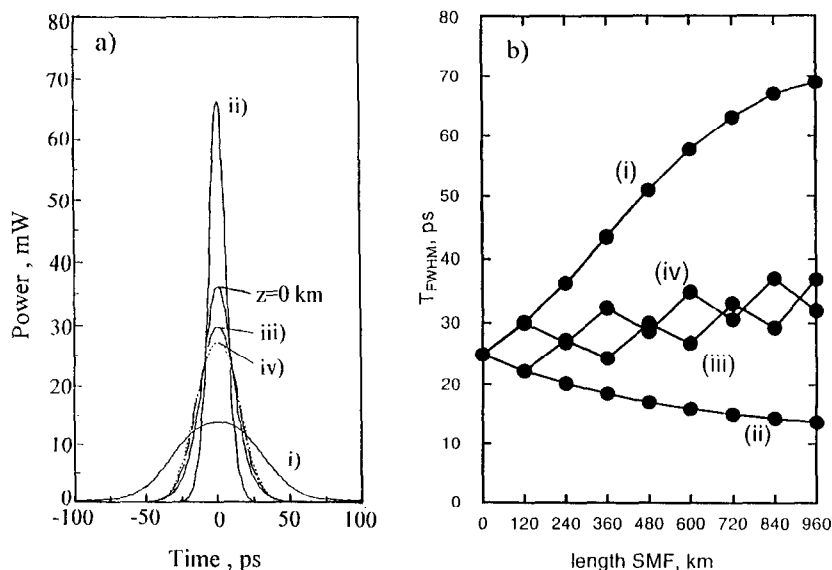


Fig. 2. Single pulse propagation for 25 ps initial pulse width and 36 mW input peak power. The pulse shapes (a) are shown for the input and output signals for different configurations including post-compensation SSSSSSSS (i), pre-compensation DDDDDDDD (ii), and alternating compensation SDSDSDS (iii) and DSDSDSDS (iv). In (b) the pulse width evolution for different configurations (the same notation as in a) is shown.

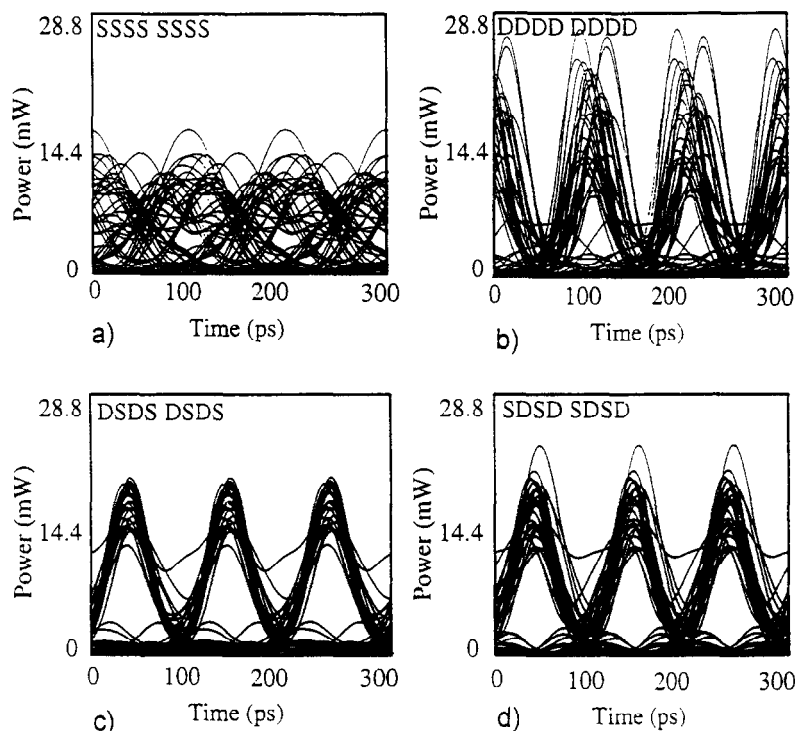


Fig. 3. Simulated eye diagrams after the 960 km SMF link for 10 Gbit/s bit rate and 36 mW peak power: (a) post-compensation (SSSSSSSS), (b) pre-compensation (DDDDDDDD); the alternating compensation schemes enabling a considerable improvement of the system performance are presented in (c) (DS DS DS DS) and (d) (SD SD SD SD).

earity. Note that the pure post- and pre-compensation schemes can be optimized by varying input pulse parameters and chirp and amplification distance. This issue will be discussed elsewhere. In the alternating compensation schemes DS DS DS DS and SD SD SD SD, however, due to the alternating effects of pulse broadening in a S-block and pulse compression in a D-block the initial signal is efficiently restored, showing that the influence of fibre nonlinearity was diminished. Furthermore, if total number of D- and S-blocks happens to be unequal due to boundary conditions in some particular practical system, pulse restoration is sufficiently achieved if the total numbers of D- and S-blocks differ just by 1. This can be seen from comparison the pulse widths for DS DS DS DS and the SD SD SD SD schemes in Fig. 2b for 120 km, 360 km, 600 km and 960 km total transmission length of the SMF, respectively.

To investigate the potential of the alternating compensation concepts we now considered pulse propagation of a bit-pattern of length  $2^7 - 1$ . In Fig. 3a, 3b the eye-diagrams are shown at the receiver output for the pure post- (a) and pre-compensation (b) schemes of the transmission line. The optical bandwidth was chosen to be 1 nm. By a suitable electrical low-pass filter (7 GHz) in the receiver a standard NRZ-detection scheme was considered. For both concepts, pure pre- and post-compensation, the eye is

closed. Again it can be seen, that pure pre-compensation leads to significant nonlinear induced pulse compression whereby in the pure post-compensation scheme the pulse are broadened and the peak power decreases. In the alternating configurations (Fig. 3c, 3d), however, the system performance is significantly improved with respect to the pure pre- and post-compensation scheme. Due to the high peak power of 36 mW no significant degradation due to ASE-noise is observable. In both alternating schemes the power penalty is about 3 dB.

In conclusion, we have studied different schemes of dispersion compensation management in cascaded transmission systems based on the standard monomode fibers. We have suggested a new system design with very low eye opening penalty at large amplifier spacings of 120 km and high input peak power over a total transmission distance of 960 km standard monomode fiber. The system performance is highly improved by alternating ordering of the compensation sections.

## References

- [1] A.D. Ellis, D.M. Spirit, *Electron. Lett.* 30 (1994) 72.
- [2] C.D. Chen, J.-M.P. Delavaux, B.W. Hakki, O. Mizuhara, T.V. Nguyen, R.J. Nuyts, K. Ogawa, Y.K. Park, R.E. Tench, L.D. Tzeng, P.D. Yeates, *Electron. Lett.* 30 (1994) 1159.

- [3] K. Oda, M. Fukutoku, M. Fukui, T. Kitoh, H. Toba, Proc. OFC'95, PD22, San Jose, USA (1995).
- [4] S. Artigaud, M. Chbat, P. Nouchi, F. Chiquet, D. Bayart, L. Hamon, A. Pitel, F. Goudeseune, P. Bousselet, J.-L. Beylat, Electron. Lett. 32 (1996) 1389.
- [5] H. Onaka, H. Miyta, G. Ishikawa, K. Otsuka, H. Ooi, Y. Kai, S. Kinoshita, M. Seino, H. Hishimoto, T. Chikama, Proc. OFC'96, PD19, San Jose, USA (1996).
- [6] N. Smith, F.M. Knox, N.J. Doran, K.J. Blow, I. Bennion, Electron. Lett. 32 (1996) 55.
- [7] I. Gabitov, S.K. Turitsyn, Optics Lett. 21 (1996) 327.
- [8] F.M. Knox, W. Forysiak, N.J. Doran, J. Lightwave Techn. 13 (1995) 1955.
- [9] F. Küppers, A. Mattheus, R. Ries, Pure Appl. Optics 4 (1995) 459.